Acta Pharmaceutica Sinica B 2022;12(9):3602–3617

Chinese Pharmaceutical Association
Institute of Materia Medica, Chinese Academy of Medical Sciences

Acta Pharmaceutica Sinica B

www.elsevier.com/locate/apsb
www.sciencedirect.com

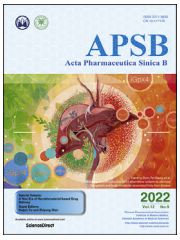

ORIGINAL ARTICLE

LncRNA *DACH1* protects against pulmonary fibrosis by binding to SRSF1 to suppress *CTNNB1* accumulation

Jian Sun[a,b,f,†], Tongzhu Jin[a,b,†], Zhihui Niu[a,b,†], Jiayu Guo[a,b,†], Yingying Guo[a,b], Ruoxuan Yang[a,b], Qianqian Wang[a,b], Huiying Gao[a,b], Yuhan Zhang[a,b], Tianyu Li[a,b], Wenxin He[c], Zhixin Li[c], Wenchao Ma[a,b], Wei Su[a,b], Liangliang Li[a,b], Xingxing Fan[d], Hongli Shan[a,b,e], Haihai Liang[a,b,e,*]

[a]*Department of Pharmacology (State-Province Key Laboratories of Biomedicine-Pharmaceutics of China, Key Laboratory of Cardiovascular Research, Ministry of Education), College of Pharmacy, Harbin Medical University, Harbin 150081, China*
[b]*Northern Translational Medicine Research and Cooperation Center, Heilongjiang Academy of Medical Sciences, Harbin Medical University, Harbin 150081, China*
[c]*Department of Thoracic Surgery, Shanghai Pulmonary Hospital, Tongji University, Shanghai 200433, China*
[d]*State Key Laboratory of Quality Research in Chinese Medicine/Macau Institute for Applied Research in Medicine and Health, Macau University of Science and Technology, Macau (SAR), China*
[e]*Research Unit of Noninfectious Chronic Diseases in Frigid Zone (2019RU070), Chinese Academy of Medical Sciences, Harbin 150081, China*
[f]*Zhuhai People's Hospital, Guangdong Provincial Key Laboratory of Tumor Interventional Diagnosis and Treatment, Zhuhai Hospital Affiliated with Jinan University, Jinan University, Zhuhai 519000, China*

Received 6 January 2022; received in revised form 4 March 2022; accepted 8 March 2022

KEY WORDS

Idiopathic pulmonary fibrosis;
LncRNA *DACH1*;
SRSF1;

Abstract Idiopathic pulmonary fibrosis (IPF) is a progressive disease with unknown etiology and limited therapeutic options. Activation of fibroblasts is a prominent feature of pulmonary fibrosis. Here we report that lncRNA *DACH1* (dachshund homolog 1) is downregulated in the lungs of IPF patients and in an experimental mouse model of lung fibrosis. *LncDACH1* knockout mice develop spontaneous pulmonary fibrosis, whereas overexpression of *LncDACH1* attenuated TGF-β1-induced aberrant activation,

*Corresponding author.
E-mail address: lianghaihai@ems.hrbmu.edu.cn (Haihai Liang).
[†]These authors made equal contributions to this work.
Peer review under responsibility of Chinese Pharmaceutical Association and Institute of Materia Medica, Chinese Academy of Medical Sciences.

https://doi.org/10.1016/j.apsb.2022.04.006

CTNNB1;
Fibroblast;
Myofibroblast;
Extracellular matrix;
Proliferation

collagen deposition and differentiation of mouse lung fibroblasts. Similarly, forced expression of *LncDACH1* not only prevented bleomycin (BLM)-induced lung fibrosis, but also reversed established lung fibrosis in a BLM model. Mechanistically, *LncDACH1* binding to the serine/arginine-rich splicing factor 1 (SRSF1) protein decreases its activity and inhibits the accumulation of *Ctnnb1*. Enhanced expression of SRSF1 blocked the anti-fibrotic effect of *LncDACH1* in lung fibroblasts. Furthermore, loss of *LncDACH1* promoted proliferation, differentiation, and extracellular matrix (ECM) deposition in mouse lung fibroblasts, whereas such effects were abolished by silencing of *Ctnnb1*. In addition, a conserved fragment of *LncDACH1* alleviated hyperproliferation, ECM deposition and differentiation of MRC-5 cells driven by TGF-β1. Collectively, *LncDACH1* inhibits lung fibrosis by interacting with SRSF1 to suppress *CTNNB1* accumulation, suggesting that *LncDACH1* might be a potential therapeutic target for pulmonary fibrosis.

1. Introduction

Pulmonary fibrosis is the end-stage outcome of a large variety of lung diseases characterized by excessive fibroblast proliferation, aberrant extracellular matrix (ECM) deposition with inflammatory injury, and destruction of tissue structure[1]. The most common disease type is idiopathic pulmonary fibrosis (IPF), a severe interstitial lung disease that leads to progressive loss of lung function, resulting in significant medical burden due to its severe clinical manifestations, poor prognosis, and high mortality[2]. Increasing evidence suggests that repeated injury to the alveolar epithelium leads to excessive accumulation of fibroblasts and extracellular matrix proteins[3], which in turn leads to scarring and diminished respiratory function. Pirfenidone and nintedanib are currently approved for the treatment of IPF, but whether these two agents can improve the survival of patients with IPF and their existing adverse drug reactions remains controversial[4]. The molecular mechanisms of IPF are not fully understood, and there is still a lack of effective treatments for IPF other than lung transplantation.

Noncoding RNAs such as microRNAs have been suggested to be involved in the development of pulmonary fibrosis[5]. Long noncoding RNAs (lncRNAs) are defined as RNA transcripts more than 200 nucleotides with little protein-coding function[6]. Initial studies identified altered expression levels of certain lncRNAs in cancer cells[7] and that these lncRNAs could serve as markers and potential drug targets for cancer diagnosis. Moreover, recent studies have reported that the lncRNAs are highly associated with drug metabolism and drug resistance[8]. Mutations and dysregulation of lncRNAs have been successively linked to various human diseases, such as cardiovascular diseases[9], neurological disorders[10], and organ fibrosis[11]. Feng et al.[12] reported that lncRNA *Erbb4-IR* produces a marked effect in renal fibrosis by targeting Smad7 in the TGF-β/Smad pathway. In our previous study we found that lncRNA *PFAR* played a corresponding role in IPF[13].

LncRNAs are able to regulate gene expression at multiple levels. In simple terms, lncRNAs are able to participate in epigenetic regulation, transcriptional regulation, as well as post-transcriptional regulation[14]. Mechanistically, lncRNAs can affect gene expression by directly binding to proteins, influencing histone modifications, interfering with mRNA splicing, sponging microRNAs, etc. Cai et al.[15] have made outstanding contributions to the study of the role of LncRNA *DACH1* (dachshund homolog 1), which could directly bind to sarcoplasmic reticulum calcium ATPase 2a (SERCA2a) and enhance its ubiquitination and degradation, leading to impairment of cardiac function. On the other hand, *LncDACH1* could also regulate the PP1A/YAP1 pathway to participate in cardiac repair and regeneration after myocardial infarction[9]. Although a large number of studies have demonstrated the essential role of lncRNAs in human diseases, the action of *LncDACH1* in IPF pathogenesis and its underlying molecular mechanism needs to be further explored.

In this study, we found that *LncDACH1* was decreased in lung of both IPF patients and bleomycin (BLM)-induced mice, suggested that *LncDACH1* may played critical roles in pulmonary fibrosis. Consistent with this finding, *LncDACH1*-KO mice exhibit lung pathological changes, collagen deposition, lung function decline and remodeling. We found that *LncDACH1* modulates serine/arginine-rich splicing factor 1 (SRSF1) protein, ultimately suppressing lung fibroblast activation.

2. Materials and methods

2.1. Mouse model

Male C57BL/6 mice aged 6−8 weeks with an average body weight of 18−23 g were used. A mouse model of pulmonary fibrosis was generated by a single intratracheal administration of BLM (3 mg/kg, Selleck) under anesthesia resulting in an experimental pulmonary fibrosis model 21 days later. Control mice received saline. Prevention and treatment groups were induced with adenovirus-associated virus 5 carrying lncRNA *DACH1* (AAV5-*LncDACH1*) at a dose of 2×10^{10} particles by intratracheal administration. Animals were randomly assigned for each experimental group. Assessors were un-blinded to group allocation. All animal experiments were approved by the Harbin Medical University College of Pharmacy Ethical committee (A-IRB3001721, China).

2.2. Cell culture and treatment

Primary mouse lung fibroblasts (PMLFs) were extracted from the lung tissues of 3-day-old mice. After digestion and filtration, the extracted PMLFs were cultured in DMEM (Biological Industries, Israel), supplemented with 10% FBS (Biological Industries, Israel), and 1% penicillin−streptomycin−amphotericin B (Solarbio, Beijing, China) under sterile conditions. The medium was changed,

non-adherent cells were removed differentially after 6 h, and further manipulations were performed when cells were well-established.

The human fetal lung fibroblast cell line MRC-5 was obtained commercially from the Cell Bank of Chinese Academy of Sciences. Cells were cultured at 37 °C in a 5% CO_2 incubator. Cells were allowed to grow and adhere to the wall. After starvation in serum-free medium for 6 h, the cells were transfected with 2 μg of plasmid followed by treatment with or without recombinant human TGF-β1 (10 ng/mL; PeproTech, USA). MRC-5 authentication was determined by short tandem repeat (STR) profiling and free from mycoplasma contamination.

Adult mouse lung fibroblasts (AMLFs) were obtained from 6−8-week-old C57/BL6 mice. Mouse lung tissues were harvested, minced into centrifuge tubes on an ultraclean table. After pancreatin digestion, the supernatant was aspirated and the reaction was terminated by adding culture medium. Pure AMLFs were filtered and placed in culture medium as described above.

2.3. Patients samples

Patient samples of IPF and non-IPF were provided by Shanghai Pulmonary Hospital. Informed consent was obtained from patients and the study was approved by the Harbin Medical University College of Pharmacy Ethical Committee (A-IRB3001721) and conformed to the Declaration of Helsinki. Patient information is displayed in Supporting Information Table S1.

2.4. Cell transfection

PMLFs/MRC-5 were transiently transfected with *LncDACH1* plasmid or small interference RNA (siRNA) of *LncDACH1*/*Srsf1*/*Ctnnb1* using Lipo2000 (Invitrogen) according to the manufacturer's instructions. SiRNA and a negative control siRNA (siNC) were synthesized by Ribobio (Guangzhou, China). SiRNA sequences are displayed in Supporting Information Table S2.

2.5. Quantitative real-time RT-PCR

Total RNA was extracted from the lung tissues, PMLFs, AMLFs and MRC-5 cells using TRIzol reagent. The concentration and purity of the RNA was determined with a NanoDrop 8000 (Thermo). cDNA reverse transcription kits (5× All-in-One RT Master Mix, TransGene Biotech, China) were used to reverse transcribe total RNA using random primers. The mRNA was quantified by SYBR Green on ABI 7500 Fast Real-time PCR system (Applied Biosystems, USA). The *GAPDH* gene was used for normalization. Primer efficiency was assessed by a series of dilutions, and a dissociation curve was used to assess the primer specificity. Primers sequences are shown in Supporting Information Table S3. The data were analyzed by $2^{-\Delta\Delta CT}$ method.

2.6. Western blot

Protein samples were extracted from cells and tissues using RIPA lysis buffer with protease inhibitor (Beyotime, Jiangsu, China). The proteins were separated on a 10% or 8% SDS polyacrylamide gel and transferred to a nitrocellulose membrane (Pall Life Sciences, Ann Arbor, MI, USA). Proteins were identified with antibodies against FN1 (1:500, Proteintech, Wuhan, China), Collagen I (1:500, Affinity Biosciences, OH, USA), SRSF1 (1:500, Proteintech, Wuhan, China), and β-catenin (1:500, Proteintech, Wuhan, China). β-Actin (1:1000, Proteintech, Wuhan, China) served as a loading control. The membranes were incubated with secondary antibodies (1:8000, Abcam, USA) for 1 h at room temperature. Finally, Odyssey (Odyssey CLX, Biosciences, USA) was used to detect and quantify protein expression.

2.7. Masson's trichrome staining and immunohistochemistry

Lung tissues were fixed in 4% paraformaldehyde (Solarbio, Beijing, China) and embedded in paraffin to prepare 5-μm tissue sections. The tissue sections were deparaffinated and rehydrated in xylene and different concentrations of ethanol. After incubation with 3% hydrogen peroxide, the sections were heated to repair antigen and cooled to room temperature. The sections were blocked with 50% normal goat serum albumin for 1 h, followed by incubation with Collagen I antibody and α-SMA antibody at 4 °C overnight. The next day, sections were incubated with horseradish peroxidase-conjugated secondary antibodies and colored by 3,3′-diaminobenzidine (ZsBio, Beijing, China). IHC analysis was measured by a fluorescence microscopy (DP80, Olympus, Japan). Hematoxylin and eosin (H&E) and Masson's trichrome staining were performed according to the instructions of the kit (Solarbio, Beijing, China), and histopathological changes were observed under a microscope.

2.8. Wound healing assay

The PMLFs or MRC-5 cells were cultured in 6-well plates overnight to determine the migratory ability of lung fibroblasts. The cell monolayer was scratched on the tip of 200 μL plastic micropipette and cultured under standard culture conditions. The cells then were transfected and observed with Nikon Ts100 microscope (Nikon, Tokyo, Japan) at 0 and 24 h.

2.9. EdU fluorescence staining

A Cell-Light EdU Apollo 567 *In Vitro* Kit (RiboBio, Guangzhou, China) was used to detect cell proliferation. PMLFs or MRC-5 cells were cultured in 24-well plates. At 48 h after transfection the experiment was carried out according to the manufacturer's protocol.

2.10. Immunofluorescence staining

Lung fibroblasts were seeded into 24-well cell culture plates. After transfection and treatment, the cells were fixed in 4% paraformaldehyde at room temperature and then solubilized and blocked. The cells were incubated with anti-α-SMA (1:200, Abcam), anti-SRSF1 (1:50, Proteintech) and anti-β-catenin (1:200, Affinity) at 4 °C overnight. On the second day, FITC-conjugated goat anti-mouse antibody (1:500, Alexa Fluor 594, Life Technology) or goat anti-rabbit antibody (1:500, Alexa Fluor 488, Life Technology) was added and incubated for 1 h in the dark condition. The nuclei were counterstained with DAPI for 5 min. Immunofluorescence was observed and analyzed under a fluorescence microscope.

For immunofluorescence of tissue cryosections, retrieved lung tissues were fixed with 4% paraformaldehyde and embedded with Tissue-Tek OCT (Sakura) at −80 °C. Six μm-thick sections were cut in a Leica cryostat at −20 °C, post-fixed in acetone, and labeled with the appropriate primary and secondary antibody.

2.11. Fluorescent in situ hybridization (FISH)

Fluorescent *In Situ* Hybridization Kit (Ribobio, Guangzhou, China) was used to detect the location of *LncDACH1*. Lung

fibroblasts were fixed in 4% paraformaldehyde and solubilized with 0.4% Triton-100 for 10 min before blocking. Under dark conditions, the cells were pre-hybridized at 37 °C for 30 min, and the lncRNA FISH probe mixture was hybridized overnight at 37 °C. The cells were then washed under different conditions, and the nuclei were stained with DAPI (Roche, Basel, Switzerland) for 5 min. Fluorescence microscopy was used to observe the samples.

2.12. *Micro computed tomography (Micro-CT) of mouse lung*

The lung tissue density of mice was quantitatively measured by CT, and the degree of pulmonary fibrosis in each group was determined. CT plain scan was performed by the following methods: after anesthesia, the mice were placed on the scanning bed and kept in a supine position, then the chest of the mice was fixed with tape, and the living lung tissue of the mice was scanned after setting the scanning parameters. The images were automatically generated by the system workstation, and the images were post-processed by the relevant system software. The structural and morphological changes of lung tissue were observed to evaluate the different degrees of pulmonary fibrosis with comparison to the control group.

2.13. *RNA pull-down*

LncDACH1 probe was labeled with biotin and co-incubated with streptavidin-coated magnetic beads to form complexes, followed by protein enrichment by co-incubation with cell lysates. After washing the beads, protein sample buffer was added and heated in boiling water for 10 min. The SRSF1 target band was detected after samples were electrophoretically separated (12.5% SDS-PAGE) and assayed by Western blotting.

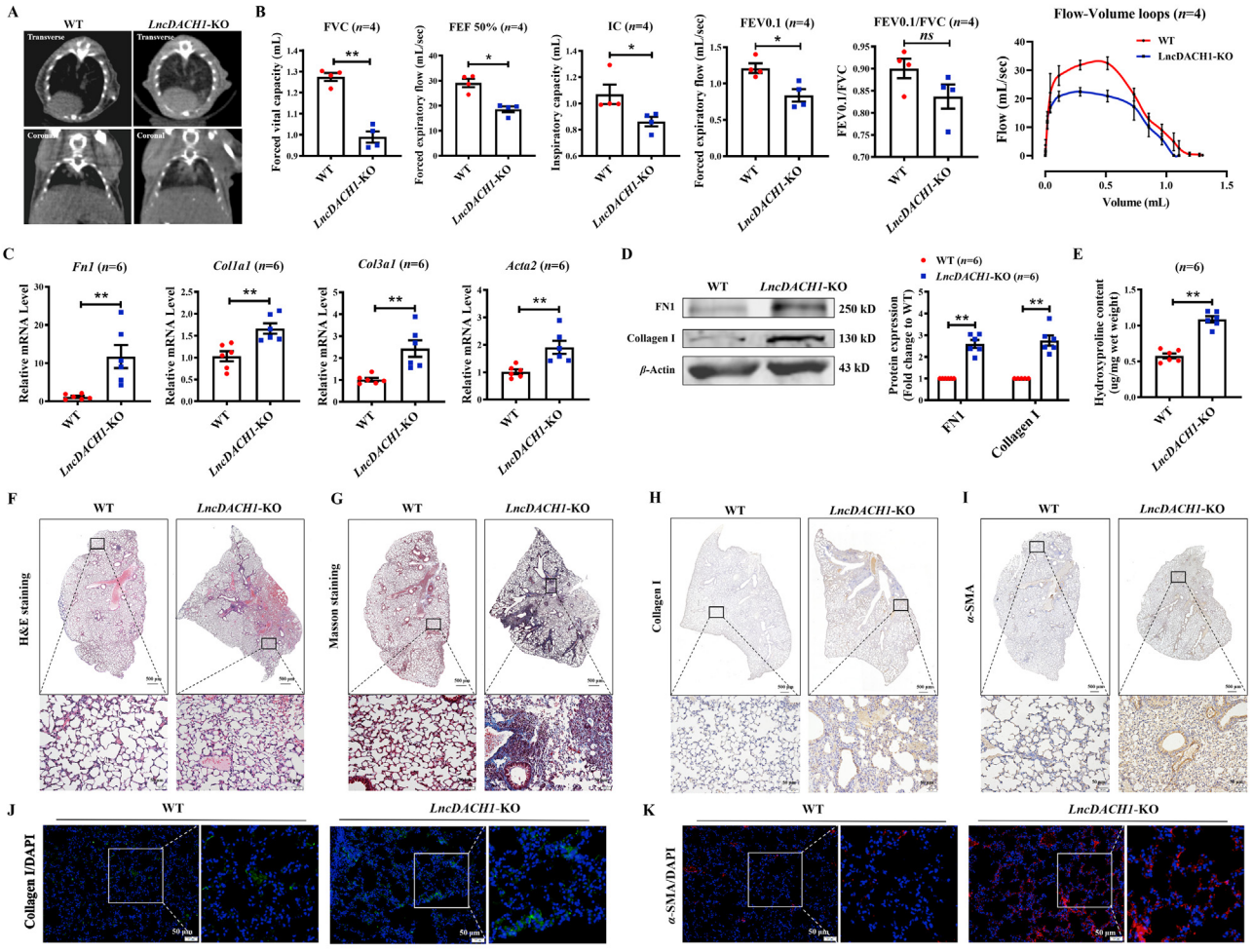

Figure 1 Loss of *LncDACH1* results in pulmonary fibrosis in mice. (A) Micro-CT shows that the shadow area of the lungs in *LncDACH1*-KO mice was significantly greater than that of WT; $n = 4$. (B) Forced vital capacity (FVC), forced expiratory flow (FEF), FEV0.1, FEV0.1/FVC, inspiratory capacity (IC) as well as Flow-volume loops were reduced in *LncDACH1*-KO mice as detected by a flexiVent system; $n = 4$. (C) qRT-PCR validated that mRNA expression of *Fn1*, *Col1a1*, *Col3a1* and *Acta2* was promoted by *LncDACH1* deficiency; $n = 6$. (D) The protein levels of FN1 and Collagen I detected by Western blot assays; $n = 6$. (E) Hydroxyproline content in *LncDACH1*-KO mice compared to WT mice; $n = 6$. (F, G) H&E and Masson staining reveal more exacerbated lung tissue morphology and increased fibrotic areas in *LncDACH1*-KO mice compared with WT mice; bar = 50 μm; $n = 3$. (H, I) Collagen I and α-SMA were increased in *LncDACH1*-KO mice as shown by immunohistochemical analysis; scale bar = 50 μm; $n = 3$. (J, K) Collagen I and α-SMA were stained by immunofluorescence analysis; bar = 50 μm; $n = 3$. Data are presented as mean ± SEM; $^*P < 0.05$, $^{**}P < 0.01$; *ns*, no significance. Micro-CT, micro computed tomography.

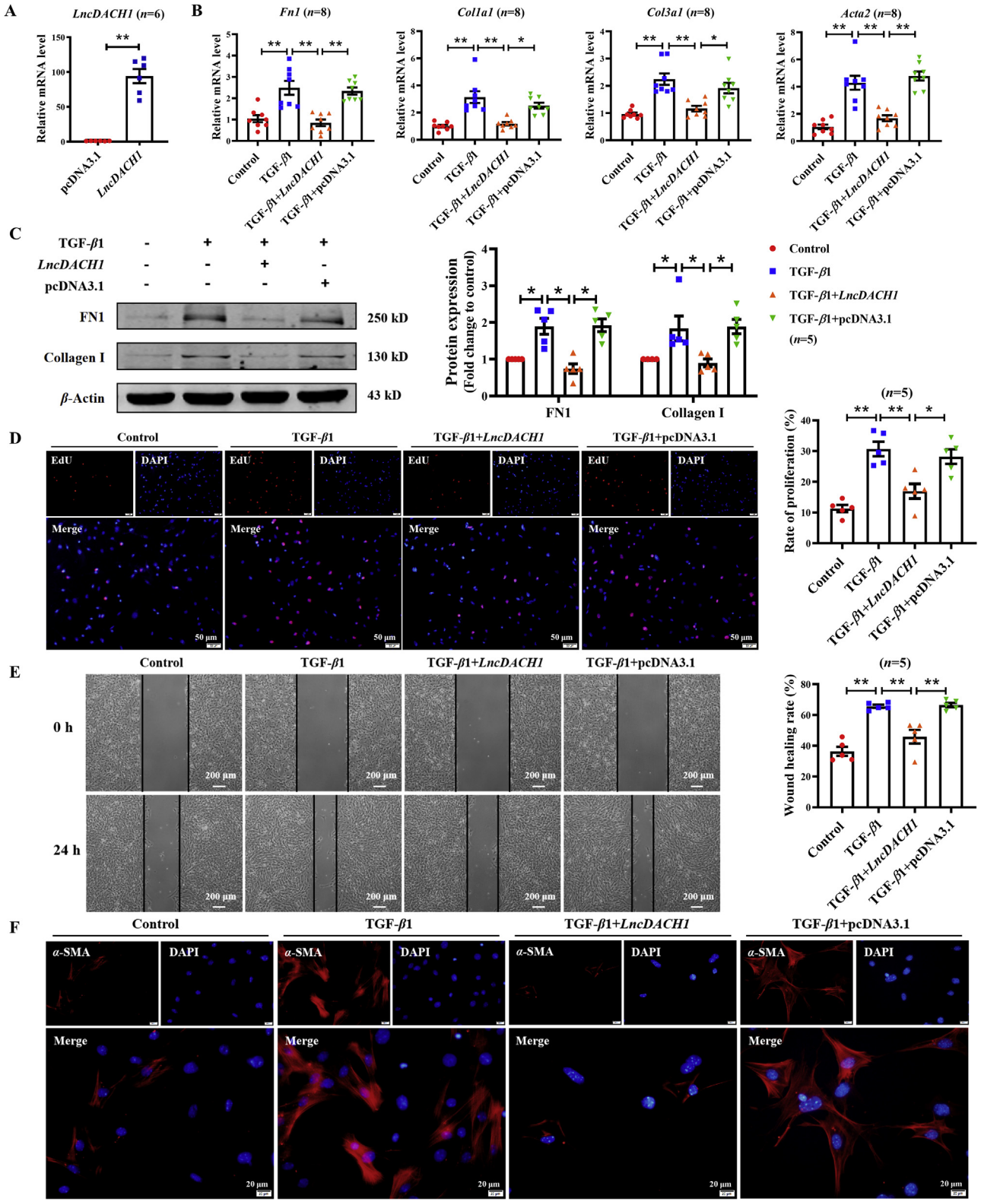

Figure 2 Anti-fibrotic effects of *LncDACH1* in primary mouse lung fibroblasts. (A) qRT-PCR analysis shows that transfected *LncDACH1* was overexpressed in PMLFs; $n = 6$. (B) The relative mRNA levels of *Fn1*, *Col1a1*, *Col3a1*, and *Acta2* in *LncDACH1*-transfected cells after TGF-β1 induction; $n = 8$. (C) *LncDACH1* inhibited the protein expression of fibrotic markers caused by TGF-β1 in PMLFs; $n = 5$. (D) The fluorescence results of an EdU assay show the proliferation of PMLFs; scale bar = 50 μm; $n = 5$. (E) The migratory ability of PMLFs was attenuated by *LncDACH1*, as detected by the wound healing assay; scale bar = 200 μm; $n = 5$. (F) Immunofluorescence staining indicated that TGF-β1-induced α-SMA positive cells were impeded by the enhanced expression of *LncDACH1* in PMLFs (scale bar = 20 μm; $n = 5$). Data are presented as mean ± SEM; $^*P < 0.05$, $^{**}P < 0.01$. PMLFs, primary mouse lung fibroblasts.

2.14. Determination of hydroxyproline

The collagen content in mouse lung tissues was assessed using the hydroxyproline method. A 45-mg tissue sample was precisely weighed and put into a test tube for hydrolysis according to the instructions of the hydroxyproline assay kit (Jiancheng, Nanjing, China). After adjusting the pH, the supernatant was taken to determine the absorbance value at 550 nm.

2.15. Protein degradation assay

PMLFs were transfected with an *LncDACH1* overexpression plasmid at 48 h with the addition of translational inhibitor cycloheximide (CHX, 50 μg/mL, Selleck, Shanghai, China) or proteasome inhibitor MG132 (50 μmol/L, Selleck, Shanghai, China), and then proteins were extracted after 0, 1, 2, and 4 h and SRSF1 degradation was assessed by Western blot assay.

2.16. Lung function measurements

Invasive pulmonary function testing was measured with the flexiVent system (flexiVent; SCIREQ, Montreal, QC, Canada). In brief, anesthetized mice were intubated and connected to a computer-controlled ventilator system (tidal volume of 10 mL/kg and frequency of 150 beats/min). Three acceptable measurements were recorded (coefficient of determination >0.95) for each mouse and the average was calculated.

2.17. RNA-binding protein immunoprecipitation (RIP)

A MagnaRIPTM RNA-Binding Protein Immunoprecipitation Kit (Millipore, USA) was used to performed RNA-binding protein immunoprecipitation (RIP) according to the manufacturer's instructions. Briefly, RIP assays were performed with SRSF1 antibody or negative control immunoglobulin G (IgG; using Millipore, USA). Cells were collected and lysed in RNA lysis buffer. Then, 5 μg of SRSF1 antibody or IgG was incubated with 50 μL of magnetic bead suspension for 30 min at room temperature to prepare the beads for immunoprecipitation. The magnetic beads were resuspended with RIP immunoprecipitation buffer and incubated with the cells at 4 °C overnight. The next day, the RNA/magnetic bead complex was washed and resuspended in proteinase K buffer to isolate proteins. The immunoprecipitated RNA was then purified for agarose gel electrophoresis or qRT-PCR analysis. IgG enrichment served as negative controls.

2.18. Statistics and analysis

Data are presented as the mean ± standard error of mean (SEM) of at least three independent experiments. Statistical significance was calculated using a two-tailed *t*-test or one-way analysis of variance (ANOVA) with a post-test Bonferroni-corrected *t*-test. $P < 0.05$ was considered a statistically significant difference. Statistical analyses were carried out using GraphPad Prism 8.0.

3. Results

3.1. LncDACH1 deficiency causes pulmonary fibrosis in mice

In previous studies, we generated *LncDACH1* knockout (*LncDACH1*-KO) mice, which exhibited a marked reduction of *LncDACH1* in the lungs (Supporting Information Fig. S1A). Unexpectedly, we observed that the lung shadow of *LncDACH1*-KO mice was increased compared with that of wild-type (WT) mice according to the results of micro computed tomography (Micro-CT, Fig. 1A). In addition, forced vital capacity (FVC), forced expiratory flow (FEF), FEV0.1, FEV0.1/FVC, inspiratory capacity (IC) as well as flow-volume loops were also attenuated in *LncDACH1*-KO mice (Fig. 1B), indicating that *LncDACH1* was closely related to the lung function of mice. We further detected that loss of *LncDACH1* induced mRNA levels of *Fn1*, *Col1a1*, *Col3a1* and *Acta2*, and protein expression of FN1 and Collagen I, which are associated with pulmonary fibrosis (Fig. 1C and D). Hydroxyproline was the most abundant in collagen, an indicator that was elevated by knockout of *LncDACH1* (Fig. 1E). Using H&E staining and Masson's trichrome staining on lung tissue sections, we observed that knockout of *LncDACH1* promoted collagen deposition and increased fibrotic area (Fig. 1F and G). Consistent with these results, immunohistochemistry and immunofluorescence confirmed the upregulated expression of Collagen I and α-SMA in the lungs of *LncDACH1*-KO mice (Fig. 1H−K), indicating that *LncDACH1*-deficient mice exhibit spontaneous pulmonary fibrosis.

To evaluate the role of *LncDACH1* in pulmonary fibrosis, we examined the expression of *LncDACH1* in lung scar foci. As shown in Fig. S1B and S1C, qRT-PCR analysis showed that the expression of *LncDACH1* was downregulated in lung tissues of IPF patients and in BLM-treated mice.

Considering the heterogeneity of cells, we performed scRNA-seq analysis of cells isolated from IPF and normal lungs. Firstly, the GSE135893 dataset[16] was analyzed by IPF Cell Atlas (http://ipfcellatlas.com/)[17]. Based on relative similarity, four cell-type groups were formed: Epithelial, Endothelial, Mesenchymal and Immune. We found the expression of *DACH1*, which is the *LncDACH1* conserved sequence, were higher in fibroblasts rather than in AT2 cells (Supporting Information Fig. S2A and S2B). ScRNA-seq results from the Human Protein Atlas website (https://www.proteinatlas.org/) showed that *DACH1* was highly expressed in endothelial cells, granulocytes cell and fibroblasts (Fig. S2C and S2D). Consistent with the results *in vivo*, *LncDACH1* expression was considerably decreased both in the lung fibroblasts isolated from BLM-induced adult mice and in the TGF-β1-induced primary mouse lung fibroblasts (PMLFs) (Fig. S2E and S2F).

3.2. Overexpression of LncDACH1 alleviates TGF-β1-induced fibrogenesis in mouse lung fibroblasts

To further understand whether *LncDACH1* acts on fibroblasts, we constructed *LncDACH1* plasmids to successfully enhance *LncDACH1* expression in PMLFs (Fig. 2A). The mRNA expression of *Fn1*, *Col1a1*, *Col3a1* and *Acta2* was upregulated in PMLFs induced by TGF-β1, but these alterations were reversed after *LncDACH1* overexpression (Fig. 2B). At the same time, the protein expression of FN1 and Collagen I was lower in *LncDACH1*-transfected PMLFs than that in TGF-β1-induced cells (Fig. 2C). Since activation of fibroblasts is an important feature of pulmonary fibrosis, we evaluated the regulatory effects of *LncDACH1* on the function of PMLFs. *LncDACH1* was confirmed to suppress the increased cell proliferation induced by TGF-β1 according to EdU fluorescence staining (Fig. 2D). The results of a wound-healing assay showed that *LncDACH1* inhibited the migratory ability of lung fibroblasts (Fig. 2E). Immunofluorescence staining also showed that the transition of fibroblasts into α-

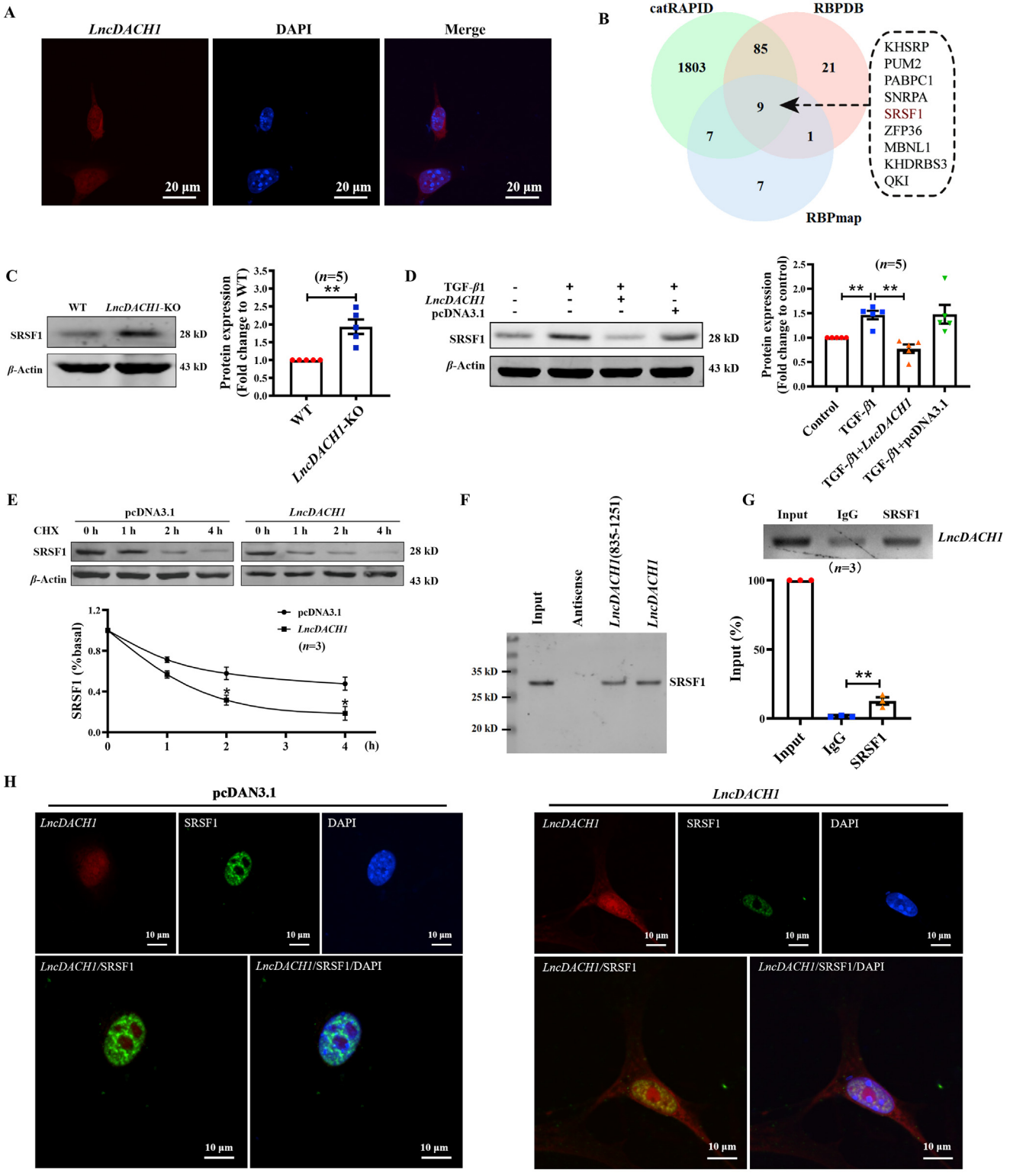

Figure 3 *LncDACH1* regulates SRSF1 expression. (A) A FISH probe demonstrates that *LncDACH1* was mainly expressed in the nucleus in PMLFs; scale bar = 20 μm; $n = 4$. (B) A Ven diagram shows the number of *LncDACH1*-binding proteins predicted by RBPmap, RBPDB and catRAPID database. (C) The protein level of SRSF1 in lung tissue of *LncDACH1*-KO mice was significantly higher than that of WT mice; $n = 5$. (D) In PMLFs, the expression of SRSF1 was regulated by *LncDACH1*; $n = 5$. (E) Cells were treated with CHX for 0, 1, 2, 4 h, respectively, to observe the degradation of SRSF1 protein by *LncDACH1*; $n = 3$. (F) The ability of *LncDACH1* full length or *LncDACH1* (835−1251) to bind SRSF1 was confirmed by RNA pull-down; $n = 3$. (G) RNA-binding protein immunoprecipitation (RIP) confirmed the interaction between *LncDACH1* and SRSF1 *in vitro*; $n = 3$. (H) FISH and immunofluorescence staining in PMLFs was performed to detect expression and localization of *LncDACH1* and SRSF1; scale bar = 10 μm; $n = 4$. Data are presented as mean ± SEM; $^*P < 0.05$; $^{**}P < 0.01$. WT, wild-type; PMLFs, primary mouse lung fibroblasts; CHX, cycloheximide.

SMA positive myofibroblasts was diminished in the presence of *LncDACH1* (Fig. 2F).

3.3. *LncDACH1 binds to SRSF1 to regulate its expression and activity*

The cellular localization of lncRNAs largely determines their mechanism of action. Therefore, we designed FISH probes and found that *LncDACH1* was expressed in both cytoplasm and nucleus, but mainly localized in the nucleus under physiological conditions (Fig. 3A). Recently, studies have reported that lncRNAs could directly bind to proteins and then regulate protein expression and activity. We hypothesized that *LncDACH1* participated in fibrogenesis by interacting with nuclear proteins. By using the RNA binding protein interaction database, including RBPmap (http://rbpmap.technion.ac.il/manual.html)[18], RBPDB (http://rbpdb.ccbr.utoronto.ca/)[19] and catRAPID (http://service.tartaglialab.com/page/catrapid_group)[20], the proteins binding with *LncDACH1* were predicted (Fig. 3B). Among the 9 predicted proteins, SRSF1 attracted our interest because it primarily binds with the *LncDACH* conserved sequence (Supporting Information Fig. S3A−S3D). As illustrated in Fig. 3C, the protein level of SRSF1 was increased in the lungs of *LncDACH1*-KO mice. PMLFs transfected with *LncDACH1* overexpression plasmid inhibited the upregulation of SRSF1 induced by TGF-β1 (Fig. 3D). In addition, we used the translational inhibitor cycloheximide to detect the effect of *LncDACH1* on SRSF1 stability in a time-dependent manner. Protein analysis showed that the overexpression of *LncDACH1* augmented the degradation of SRSF1 protein (Fig. 3E). Moreover, the proteasome inhibitor MG132 did not inhibit degradation of SRSF1 (Supporting Information Fig. S4A), and there was no significant change in the amount of ubiquitin protein binding to SRSF1 in the control group and the overexpressed *LncDACH1* group (Fig. S4B). These results indicate that *LncDACH1* does not rely on the proteasome or ubiquitination to degrade SRSF1. We next performed an RNA pull-down assay to explore whether *LncDACH1* directly bound to SRSF1. As expected, protein expression of SRSF1 was detected by Western blotting after extraction of RNA−protein complexes (Fig. 3F). An RNA binding protein immunoprecipitation (RIP) assay was carried out to evaluate the relationship between *LncDACH1* and SRSF1. We observed an enrichment of *LncDACH1* in the anti-SRSF1 antibody precipitates compared with the IgG precipitates (Fig. 3G). Moreover, overexpression *LncDACH1* visibly attenuated the SRSF1 fluorescence in PMLFs (Fig. 3H). Taken together, our results show that *LncDACH1* binds to SRSF1 to regulate its expression.

3.4. *SRSF1 is necessary for the anti-fibrotic effects of LncDACH1*

To investigate the role of the *LncDACH1* interaction with SRSF1 in lung fibrosis, we simultaneously transfected an *LncDACH1* overexpression plasmid and an adenovirus-containing *SRSF1* overexpression plasmid (Adv-*SRSF1*) into PMLFs. The infection efficiency of Adv-*SRSF1* was determined (Supporting Information Fig. S5A). At the mRNA level, enhanced expression of *SRSF1* inhibited the negative regulation of *LncDACH1* on *Fn1*, *Col1a1*, *Col3a1*, and *Acta2* (Fig. 4A). *SRSF1* also exhibited a promoting effect on the protein expression of FN1 and Collagen I (Fig. 4B), indicating that the inhibitory effect of *LncDACH1* on fibrosis and collagen deposition was restored by the expression of *SRSF1*. Likewise, PMLFs with increased SRSF1 showed stronger proliferative ability compared with *LncDACH1*-overexpressing cells (Fig. 4C). In the context of TGF-β1, *SRSF1* impeded the inhibitory effect of *LncDACH1* on cell migration and promoted the transition of fibroblasts into myofibroblasts (Fig. 4D and E). These findings suggest that SRSF1 acts as a downstream target gene of *LncDACH1*, and mediates the antifibrotic effect of *LncDACH1*.

3.5. *LncDACH1 inhibits Ctnnb1 expression by targeting SRSF1*

Previous studies have shown that SRSF1 promotes β-catenin protein accumulation by recruiting *Ctnnb1* mRNA and enhancing its biosynthesis[21]. *Ctnnb1* is a key effector of the Wnt signaling pathway and is involved in the pathogenesis of pulmonary fibrosis[22]. We took lung tissues from *LncDACH1*-KO mice for Western blot assays and found significant upregulation of the β-catenin protein level (Fig. 5A). Subsequently, we found that *LncDACH1* could reverse the increased β-catenin expression induced by TGF-β1 *in vitro* (Fig. 5B). However, the suppression of β-catenin protein by *LncDACH1* was abolished with *SRSF1* overexpression (Fig. 5C). Moreover, immunofluorescent staining showed that forced expression of *LncDACH1* inhibited the expression and nuclear translocation of β-catenin in TGF-β1-treated PMLFs, whereas this effect was significantly attenuated by *SRSF1* overexpression (Fig. 5D).

Next, we constructed small interfering RNAs (siRNAs) to silence *LncDACH1* and *Ctnnb1* and verified their efficiency (Supporting Information Fig. S5B and S5C). As illustrated in Fig. 5E, silencing of *LncDACH1* promoted the expression and nuclear translocation of β-catenin, whereas this effect was markedly inhibited by *Ctnnb1* knockdown. qRT-PCR results showed that *LncDACH1* deficiency led to the upregulation of *Fn1*, *Col1a1*, *Col3a1*, and *Acta2*, while silencing *Ctnnb1* reversed the above changes (Fig. 5F). Knockdown of *Ctnnb1* inhibited the increased protein expression of FN1, Collagen I, SRSF1 and β-catenin caused by *LncDACH1* deficiency (Fig. 5G). In addition, *LncDACH1* knockdown was sufficient to induce the proliferation and migration of PMLFs, which was abolished by knockdown of *Ctnnb1* (Fig. 5H and I). According to the results of immunofluorescence, the expression of α-SMA was increased in *LncDACH1*-silenced cells, while the inhibition of *Ctnnb1* reversed the differentiation of fibroblasts into myofibroblasts (Fig. 5J). Transfection with si-*LncDACH1* promoted β-catenin expression, and si-*Srsf1* co-expression attenuated expression (Supporting Information Fig. S6). Thus, our data reveal that *Ctnnb1* is a key step in the regulation of lung fibrosis by *LncDACH1*-targeting of SRSF1.

3.6. *Enhanced expression of LncDACH1 prevents BLM-induced pulmonary fibrosis in mice*

To verify whether *LncDACH1* exerts anti-fibrotic effects *in vivo*, we constructed an adenovirus associated virus 5 (AAV-5) overexpression plasmid containing *LncDACH1*, named AAV5-*LncDACH1*. We administered AAV5-*LncDACH1* intratracheally 14 days before BLM induction to observe the preventative effect of *LncDACH1* on lung fibrosis. Mice were euthanized on Day 21 after BLM injection and lung tissues were obtained for subsequent studies (Fig. 6A). *LncDACH1* increased in the lungs of AAV5-*LncDACH1*-treated mice and decreased in the lungs of BLM-treated mice (Supporting Information Fig. S7A). According to qRT-PCR analysis, the mRNA levels of *Fn1*, *Col1a1*, *Col3a1* and *Acta2* were suppressed by prophylactic *LncDACH1* (Fig. 6B).

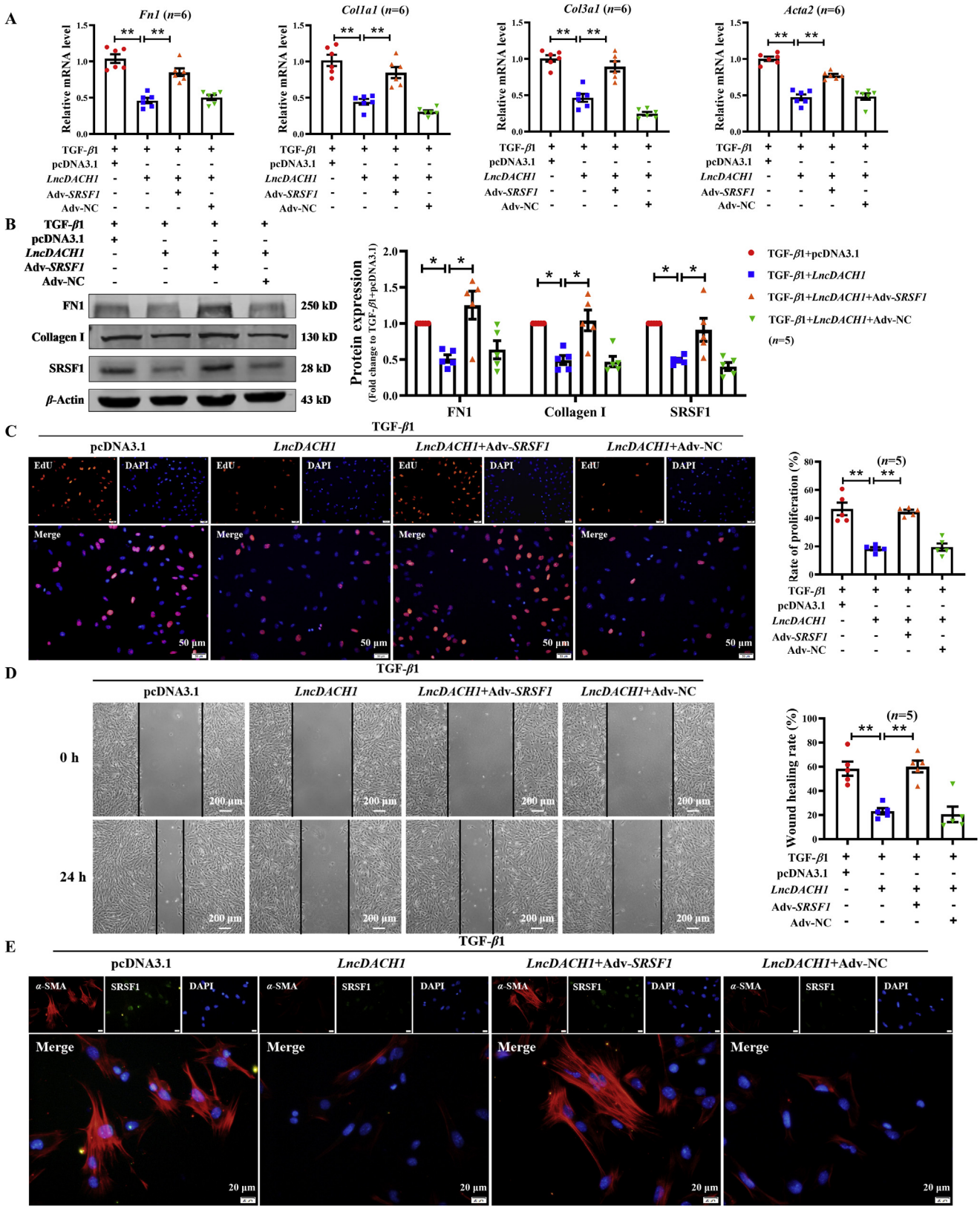

Figure 4 Overexpression of *SRSF1* limits *LncDACH1* function. (A) qRT-PCR results indicate that the overexpression of *SRSF1* normalized the inhibitory effect of *LncDACH1* on the mRNAs of fibrosis-related genes; $n = 6$. (B) Protein expression of FN1, Collagen I and SRSF1 after simultaneous overexpression of *LncDACH1* and *SRSF1*; $n = 5$. (C) EdU results (scale bar = 50 μm; $n = 5$) and (D) wound healing assays (scale bar = 200 μm; $n = 5$) show the proliferation and migration of PMLFs after Adv-SRSF1 and *LncDACH1* treatment. (E) Immunofluorescence analysis shows that *LncDACH1* inhibited the transition of fibroblasts into myofibroblasts by suppressing the expression of SRSF1. This effect of *LncDACH1* was abolished after overexpression of SRSF1. Scale bar = 20 μm; $n = 5$. Data are presented as mean ± SEM; $^{*}P < 0.05$; $^{**}P < 0.01$. Adv-*SRSF1*, *SRSF1* overexpression adenovirus.

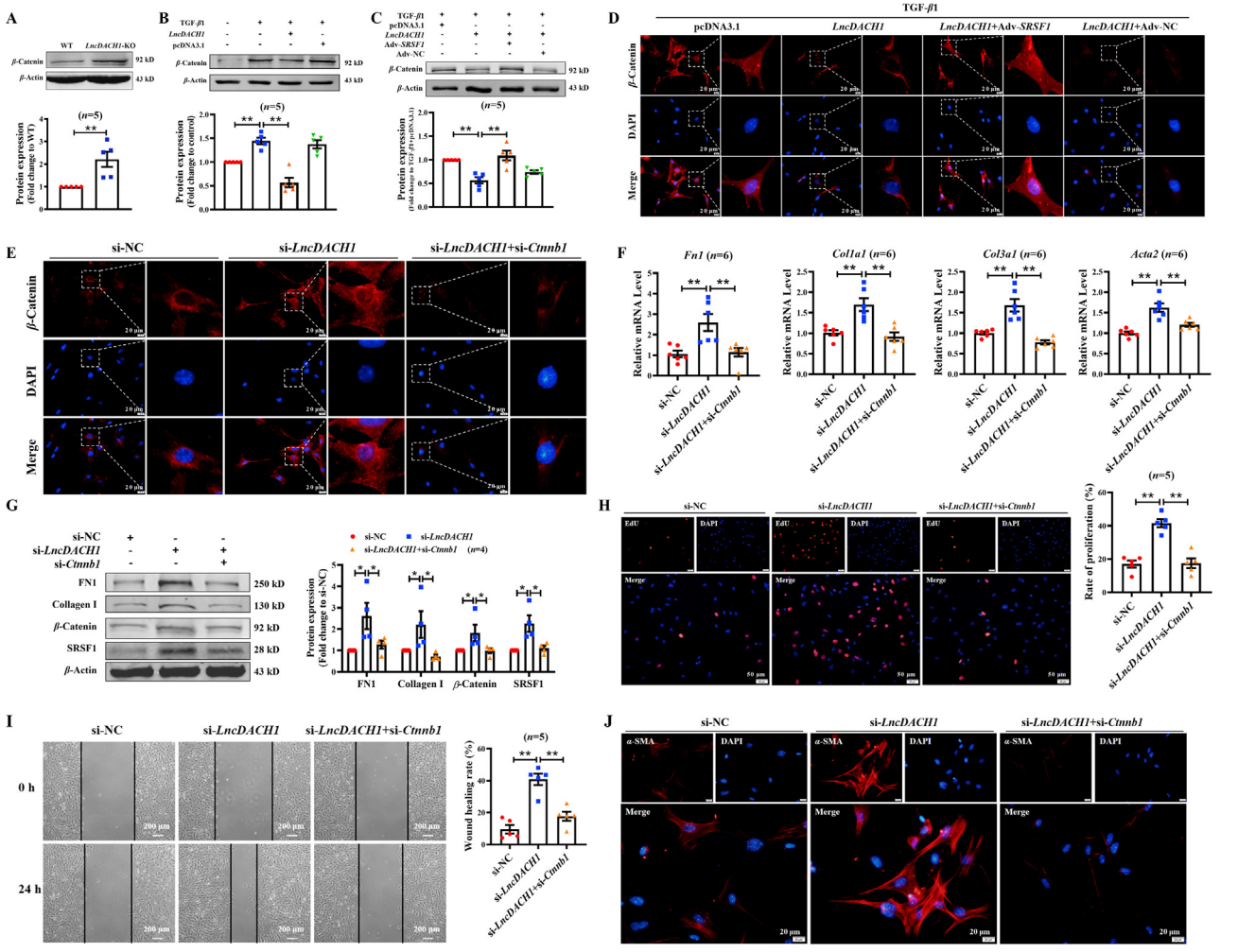

Figure 5 Silencing *Ctnnb1* abolishes the pro-fibrotic effect of *LncDACH1* deficiency. (A) The protein levels of β-catenin were dramatically increased in *LncDACH1*-KO mice; $n = 5$. (B) Western blot analysis shows that *LncDACH1* influenced the expression of β-catenin in PMLFs after TGF-β1 treatment; $n = 5$. (C) At the protein level, the negative regulation of β-catenin by *LncDACH1* was reversed by Adv-*SRSF1*; $n = 5$. (D) SRSF1 suppressed the regulation of *LncDACH1* on the expression and nuclear translocation of β-catenin; $n = 5$. (E) Silencing *LncDACH1* increased the expression and nuclear translocation of β-catenin; scale bar = 20 μm; $n = 5$. (F) As detected using qRT-PCR, knockdown of *LncDACH1* promoted the mRNA expression of *Fn1*, *Col1a1*, *Col3a1*, and *Acta2*, while this effect was alleviated by *Ctnnb1* silencing; $n = 6$. (G) The protein expression of FN1, Collagen I, β-catenin and SRSF1 were inhibited by *Ctnnb1* deficiency, as assessed by Western blots; $n = 4$. (H, I) Since *LncDACH1* was silenced, proliferation (scale bar = 50 μm; $n = 5$) and migration (scale bar = 200 μm; $n = 5$) were enhanced, whereas these effects were clearly abolished after si-*Ctnnb1*. (J) The differentiation of fibroblasts into myofibroblasts was enhanced by *LncDACH1* siRNA but abolished after transfection of *Ctnnb1* siRNA; scale bar = 20 μm; $n = 5$. Data are presented as mean ± SEM; $^*P < 0.05$; $^{**}P < 0.01$. WT, wild-type; PMLFs, primary mouse lung fibroblasts.

Western blots detected that FN1 and Collagen I induction by BLM was impeded by AAV5-*LncDACH1* (Fig. 6C). In addition, SRSF1 and β-catenin, the downstream targets of *LncDACH1*, were similarly downregulated (Fig. 6C). Hydroxyproline content in lung tissues of AAV5-*LncDACH1*-treated mice was lower compared with that in AAV5-pcDNA3.1-treated mice after treatment with BLM (Fig. 6D). After the lung tissues were fixed with paraformaldehyde and subjected to H&E and Masson staining, the mice injected with AAV5-*LncDACH1* in advance showed obvious improvement in lung tissue morphology and fibrotic area, indicating that *LncDACH1* inhibited fibrogenesis *in vivo* (Fig. 6E and F). As shown by immunohistochemistry and immunofluorescence, the increased expression of Collagen I and α-SMA induced by BLM was significantly inhibited by *LncDACH1* prevention (Fig. 6G–J). These results illustrate that *LncDACH1* plays a protective role in BLM-induced pulmonary fibrosis.

3.7. Forced expression of LncDACH1 attenuates the progression of lung fibrosis in an established experimental model of lung fibrosis in mice

Because of the complex triggers and long disease duration of pulmonary fibrosis, early awareness and treatment are effective ways to improve survival. In the therapeutic protocol, we injected AAV5-*LncDACH1* five days after BLM induction and sacrificed the mice 21 days after BLM intratracheal administration (Fig. 7A). *LncDACH1* was overexpressed in the lungs of mice treated with AAV5-*LncDACH1* (Fig. S7B). The experimental

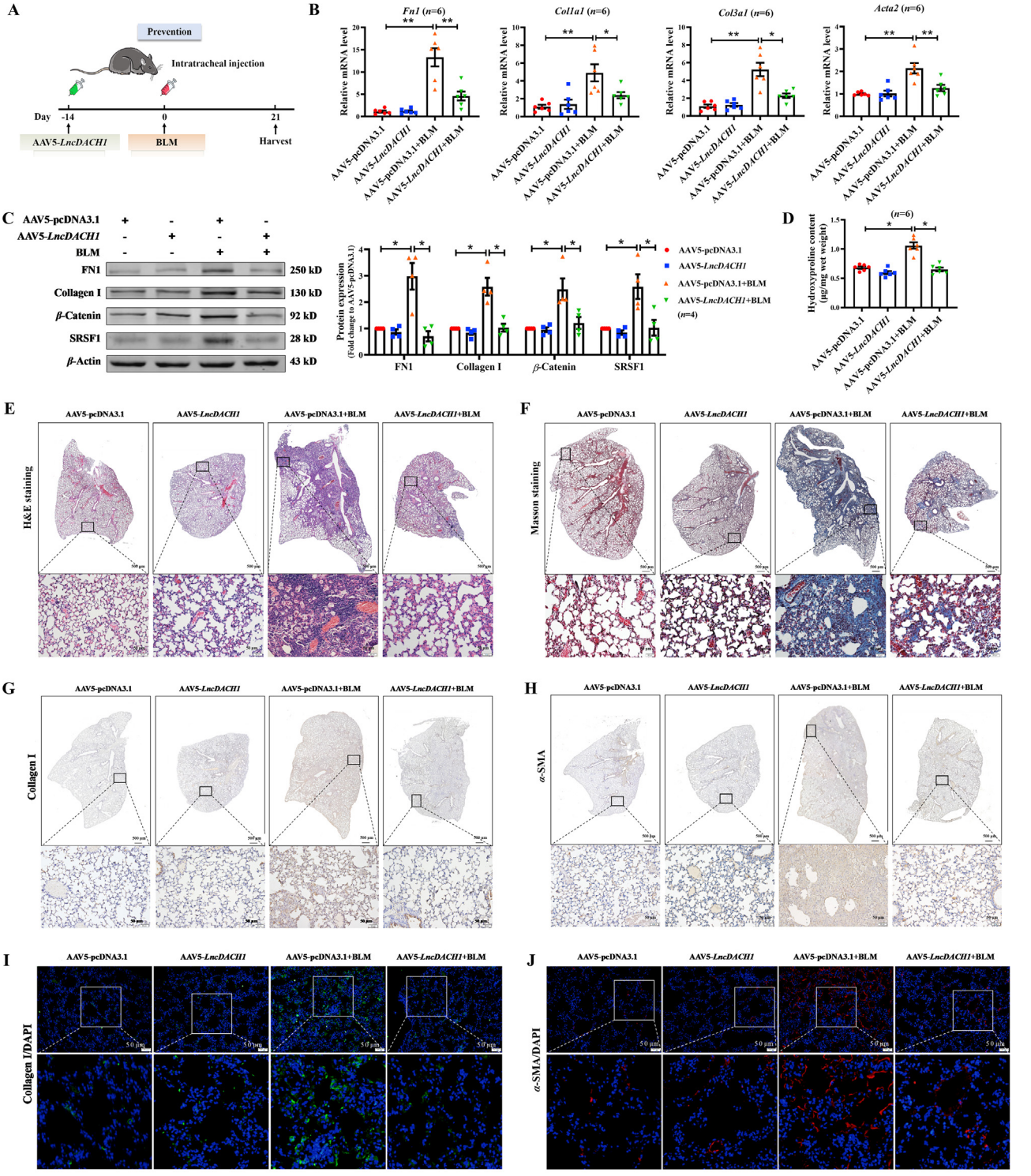

Figure 6 BLM-induced lung fibrosis is suppressed by *LncDACH1*. (A) Diagram of the animal experimental model of preventive *LncDACH1*. Mice received AAV5-*LncDACH1* intratracheally 14 days before BLM induction, and lung tissues were harvested 21 days later. (B) The relative expression of fibrosis-related genes induced by BLM was suppressed by prior administration of AAV5-*LncDACH1*; $n = 6$. (C) The effect of *LncDACH1* on the protein levels of FN1, Collagen I, β-catenin and SRSF1 *in vivo* was assessed by Western blotting; $n = 4$. (D) Hydroxyproline content was significantly reduced in the lungs of AAV5-*LncDACH1*-treated mice; $n = 6$. (E, F) H&E and Masson staining indicated that advance treatment with *LncDACH1* inhibited BLM-induced lung morphological changes and the increase in fibrotic area; scale bar = 50 μm; $n = 3$. (G–J) Immunohistochemical experiments and immunofluorescent staining detected lighter staining for Collagen I and α-SMA in *LncDACH1*-treated BLM-mice; scale bar = 50 μm; $n = 3$. Data are presented as mean ± SEM; $^*P < 0.05$; $^{**}P < 0.01$. BLM, bleomycin; AAV5-*LncDACH1*, adenovirus-associated viruses 5 containing LncRNA *DACH1*.

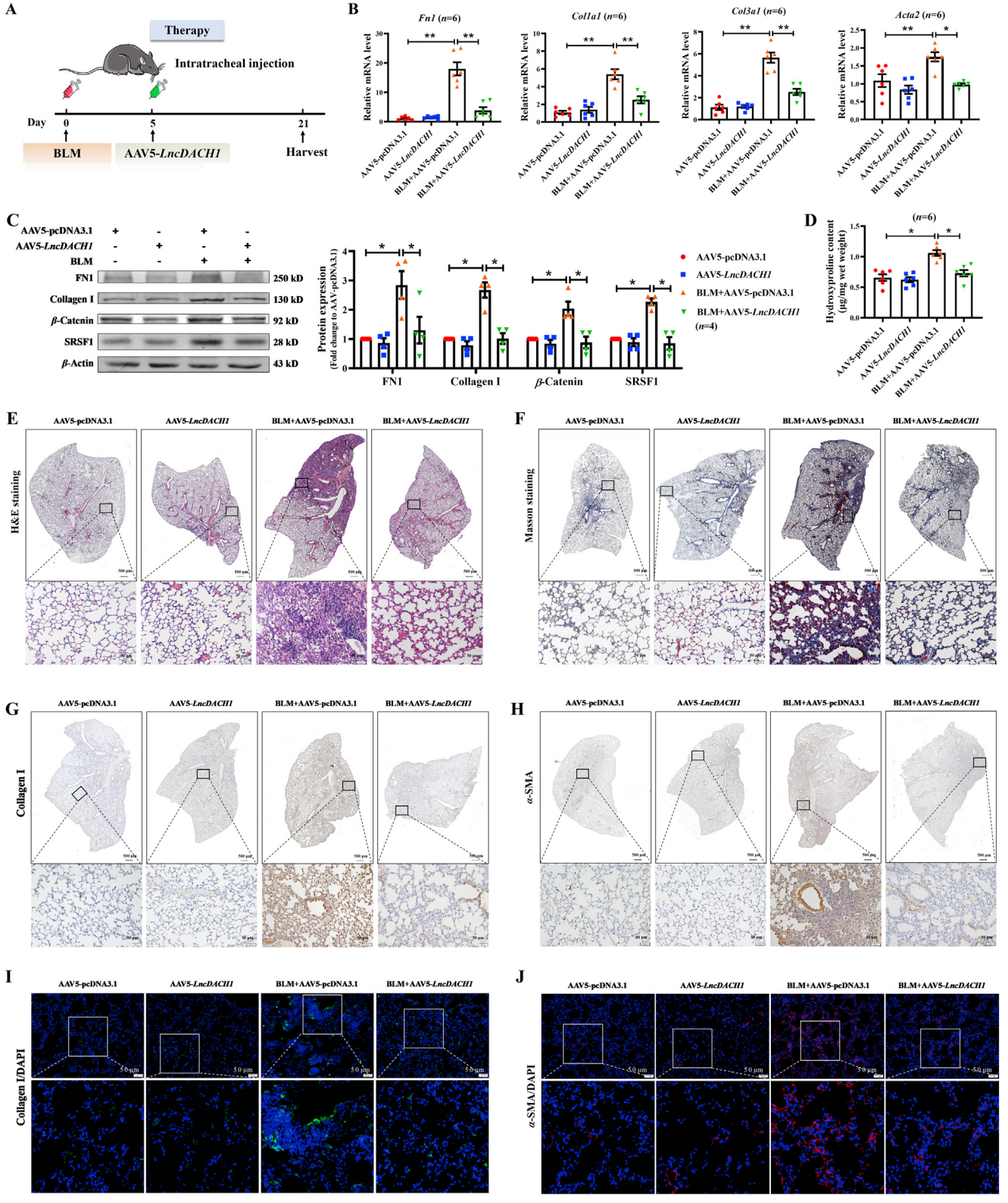

Figure 7 Inhibitory effect of therapeutic *LncDACH1* on pulmonary fibrosis. (A) Diagram of the animal experimental model of therapeutic *LncDACH1*. Mice were intratracheally administered AAV5-*LncDACH1* on Day 5 after induction by BLM and euthanized 21 days later. To observe the ameliorative effect of *LncDACH1* on lung fibrosis progression. (B) mRNA levels of the fibrosis markers, *Fn1*, *Col1a1*, *Col3a1*, and *Acta2*, after *LncDACH1* treatment; $n = 6$. (C) After fibrosis formation, *LncDACH1* inhibited the relative protein expression of FN1, Collagen I, β-catenin and SRSF1; $n = 4$. (D) BLM increased hydroxyproline content, which was reversed upon AAV5-*LncDACH1* treatment; $n = 6$. (E, F) Therapeutic *LncDACH1* alleviated BLM-induced fibrotic changes in lung tissue; scale bar = 50 μm; $n = 3$. (G–J) Immunohistochemical staining and immunofluorescent staining show that AAV5-*LncDACH1* regulated the expression of Collagen I and α-SMA in lung tissues; scale bar = 50 μm; $n = 3$. Data are presented as mean ± SEM; $^*P < 0.05$; $^{**}P < 0.01$. AAV5-*LncDACH1*, adenovirus-associated viruses 5 containing LncRNA *DACH1*.

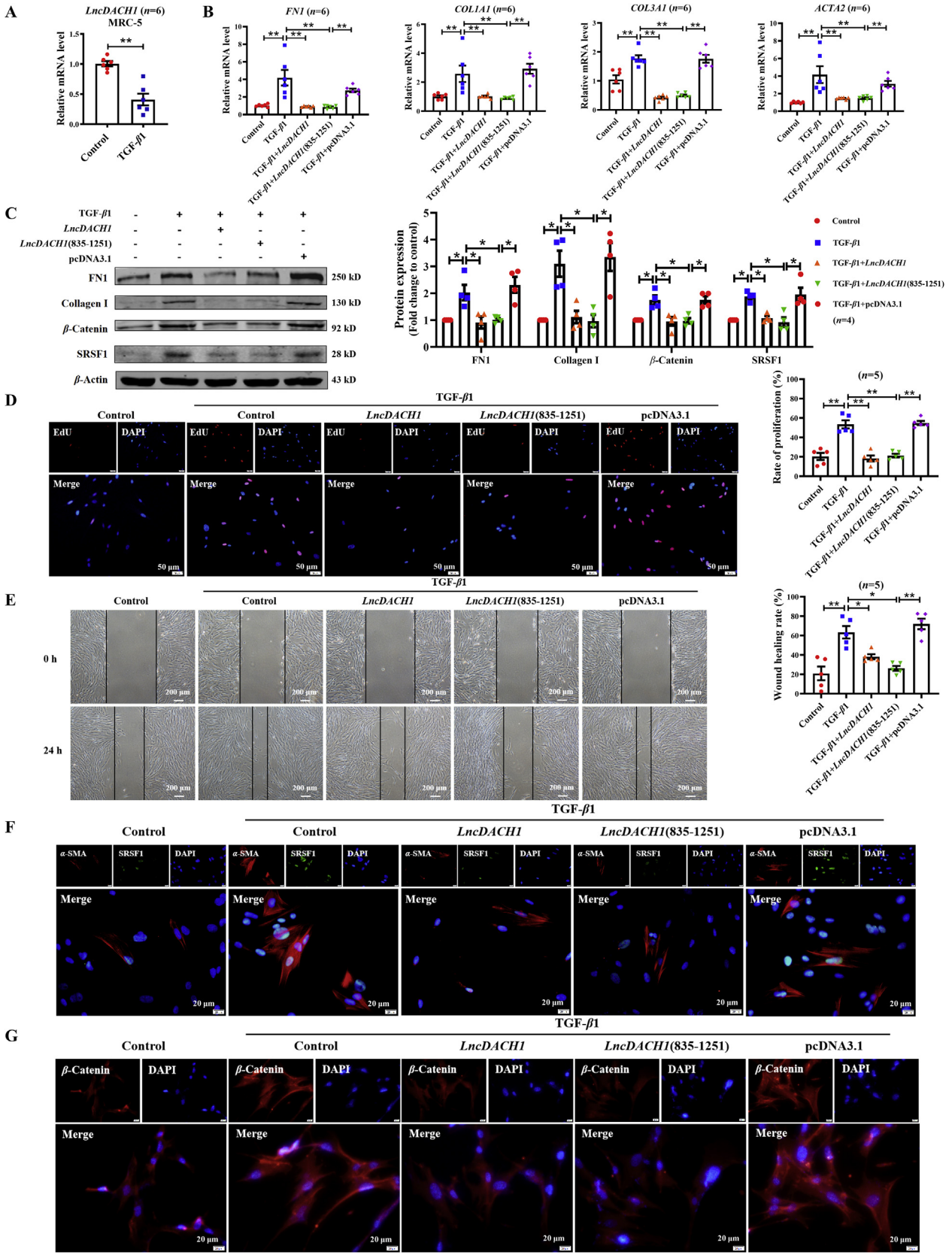

Figure 8 Effects of the conserved sequence of *LncDACH1* on human lung fibroblasts (MRC-5). (A, B) As shown in the qRT-PCR experiments, the suppression of mRNA expression of fibrosis markers by *LncDACH1*(835−1251) was consistent with that of full length *LncDACH1*; $n = 6$. (C) In MRC-5 cells, *LncDACH1*(full-length) and *LncDACH1*(835−1251) showed obvious inhibitory effects on TGF-β1-induced upregulation of FN1, Collagen I, β-catenin and SRSF1 at the protein levels; $n = 4$. The proliferation and migration of MRC-5 cells was detected by (D) EdU

results are consistent with the preventative regimen. After BLM induction of pulmonary fibrosis in mice, the mRNA and protein levels of fibrosis-related genes were suppressed by the enhanced expression of *LncDACH1* (Fig. 7B and C). The protein expression of SRSF1 and β-catenin was similarly regulated by *LncDACH1* treatment (Fig. 7C). Hydroxyproline content was not obviously different from normal control mice after *LncDACH1* treatment, but significantly decreased in mice exposed to BLM (Fig. 7D). In response to therapeutic AAV5-*LncDACH1* treatment, the lung tissues of mice showed less fibrotic area, lighter Collagen I and α-SMA staining (Fig. 7E−J), indicating that *LncDACH1* is able to impede the progression of lung fibrosis. What's more, we concurrently overexpressed *LncDACH1* and *SRSF1* in mice. Our results reveal that *LncDACH1* attenuated BLM-induced fibrosis in mice, and SRSF1 reversed the function of *LncDACH1* (Supporting Information Fig. S8). These results demonstrate the antifibrotic effects of the *LncDACH1*/SRSF1/*Ctnnb1* axis.

3.8. *Anti-fibrotic role of the conserved sequence of LncDACH1 in MRC-5 cells*

LncDACH1 exhibited potent protective effects against pulmonary fibrosis in a mouse model and in primary mouse lung fibroblasts. We wished to determine if *LncDACH1* also had the same effect on human derived fibroblasts (MRC-5 cells). Since the excessively long nucleotide sequence of *LncDACH1* limits its medicinal potential, we identified a sequence of *LncDACH1*(800−1200) likely to bind to SRSF1 (shown in Fig. 3B), based on a previous study that showed that the *LncDACH1*(835−1251) fragment is functional and highly conserved. We detected SRSF1 and *LncDACH1* (835−1251) interaction by RNA-pull down assay (Fig. 3H). qRT-PCR analysis showed that *LncDACH1*(835−1251) expression was suppressed in MRC-5 cells after induction by TGF-β1 (Fig. 8A). With regard to fibrogenesis, *LncDACH1*(835−1251) significantly alleviated TGF-β1 increased mRNA expression of *FN1*, *COL1A1*, *COL3A1* and *ACTA2*, while suppressing the up-regulated protein level of FN1, Collagen I, β-catenin and SRSF1, and the efficiency was consistent with that of full-length *LncDACH1* (Fig. 8B and C). In addition, we found that the *LncDACH1*(835−1251) inhibited migration, proliferation and differentiation of MRC-5 cells (Fig. 8D−F). Immunofluorescence assays showed that *LncDACH1*(835−1251) inhibited the activity of β-catenin by reducing its nuclear translocation (Fig. 8G). In summary, we have demonstrated that the conserved sequence of *LncDACH1* has an ameliorative effect on the activation of human fetal lung fibroblasts.

4. Discussion

In the present study, we found that *LncDACH1* was downregulated in lung tissues of IPF patients and in BLM-treated mice, and *LncDACH1*-KO mice spontaneously exhibit pulmonary fibrosis. Mechanistically, we further show that *LncDACH1* modulated *Ctnnb1* expression by targeting SRSF1, ultimately suppressing lung fibroblast differentiation and ECM deposition. Moreover, we identified the anti-fibrotic effects of *LncDACH1 in vivo*, providing a potential preventive and therapeutic target for IPF.

A growing understanding of IPF processes suggests that the heterogeneity analyses in cells contributes to mechanistic exploration. Due to the limitation of single cell sequencing in the detection of lncRNA, we analyzed the human *DACH1* (*LncDACH1* conserved sequence) expression in different cell types. The results suggest that *DACH1* is mainly enriched in fibroblasts and endothelial cells. Also, the successful clinical trials of pirfenidone and nintedanib, FDA-approved antifibrosis agents, highlight the importance of the epithelial cells and fibroblasts in pulmonary fibrosis[23,24].

We used mouse lung fibroblasts and human fetal lung fibroblast MRC-5 cells to investigate the underlying mechanism of *LncDACH1*, and found that *LncDACH1* can inhibit the activation of lung fibroblasts by negatively regulating the expression and activity of SRSF1. We validated *Ctnnb1* as a downstream target of SRSF1 in fibroblasts, and the upregulation of SRSF1 promoted β-catenin protein expression. As expected, overexpression of SRSF1 alleviated the protective effect of *LncDACH1* against fibrogenesis, both in PMLFs and in MRC-5. Correspondingly, the knockdown of *Ctnnb1* rescued the fibrogenesis triggered by *LncDACH1* silencing. We carried out an in-depth study on the protective effect of *LncDACH1* and found that whether used for treatment or prevention, *LncDACH1* could attenuate the extent and progression of pulmonary fibrosis in BLM-induced mice. Based on the present results, we demonstrate that the *LncDACH1*/SRSF1/*CTNNB1* pathway plays a crucial role in pulmonary fibrosis and may be a novel drug target.

LncDACH1 initially attracted attention because its upregulation in the failing hearts of humans and mice[15]. Many studies have confirmed the crucial role of lncRNAs. A clinical analysis by Song et al.[25] demonstrated that *LncITPF* could be used as a diagnostic marker for IPF patients. Some of our previous studies of lncRNAs in pulmonary fibrosis have focused on lncRNAs as ceRNAs to regulate miRNAs, which in turn affect the expression of downstream target genes. A previous study from our group has reported that enhanced expression of lncRNA *PFAR* promotes lung fibrosis by targeting *miR-138*/*YAP1*-*Twist* axis[13]. However, the functions of lncRNAs are considered to be more complex and diverse. Since *LncDACH1* expression is mainly localized in the nucleus in fibroblasts, we predicted proteins that are likely to have the potential to bind to *LncDACH1* using the catRAPID, RBPmap and RBPDB database, in which we focused on the splicing factor SRSF1, and the above observations were further confirmed by RNA pull-down assay. Our work reveals for the first time that *LncDACH1* competitively binds to SRSF1 in lung fibroblasts, and thereby inhibits fibroblast proliferation and differentiation, ameliorating pulmonary fibrosis.

SRSF1 is a classical member of the SR protein family, which as a regulator of alternative splicing can produce different mRNA isoforms[26]. The necessity of the SRSF1 protein was illustrated as early as 2007 when it was reported that mice with a complete knockout of SRSF1 are embryonic lethal[27]. Subsequently, an increasing number of studies have found that SRSF1 is upregulated in a variety of cancers and plays a regulatory role in the immune system[28]. Reduced expression of SRSF1 enhances the sensitivity of lung cancer cells to radiotherapy[29]. In our study, we found that SRSF1 is increased in a pulmonary fibrosis model

(scale bar = 50 μm; $n = 5$) and (E) wound healing (scale bar = 200 μm; $n = 5$) experiments; the full-length and conserved sequence of *LncDACH1* hindered the inductive effects of TGF-β1. (F) Immunofluorescence analysis revealed that *LncDACH1*(full length) and *LncDACH1*(835−1251) regulated the generation of α-SMA-positive cells in human fetal lung fibroblasts; scale bar = 20 μm; $n = 5$. (G) Distribution of β-catenin in MRC-5 cells after *LncDACH1*(835−1251) treatment; scale bar = 20 μm; $n = 5$. Data are presented as mean ± SEM; $^*P < 0.05$; $^{**}P < 0.01$.

in vivo, and overexpression of SRSF1 promotes the activation of lung fibroblasts. With the further understanding of SRSF1, it has been found that SRSF1 is not only involved in alternative splicing but also closely relate to mRNA transcription, nuclear output, translation, and protein sumoylation[28,30]. According to research from Fu et al.[21], SRSF1 can enhance the biosynthesis of *CTNNB1*, leading to the accumulation of β-catenin protein, thus leading to tumorigenesis. *CTNNB1* is an essential part of the Wnt signaling pathway and also plays an important role in fibrosis[31]. Therefore, as a downstream target of SRSF1, *CTNNB1* has attracted our attention. Here, we found that the enhanced expression of SRSF1 increases the protein level of β-catenin, which further leads to the upregulation of fibrosis-relevant genes. However, the function of SRSF1 in fibrotic diseases is just beginning to be recognized.

The risk factors of IPF are very complex, and with the background of the COVID-19 pandemic, some studies have suggested that pulmonary fibrosis may be a serious consequence of SARS-CoV-2 infection[32]. Therefore, it is more urgent to develop anti-pulmonary fibrosis drugs. Based on our results, we believe that *LncDACH1*/SRSF1/*CTNNB1* may become a new target for the prevention or treatment of pulmonary fibrosis. In recent years, drugs and other novel agents have been found to alleviate a variety of diseases by targeting lncRNAs. Sprangers et al.[33] used liposomal spherical nucleic acid, which showed dose-dependent inhibition of lncRNA *Malat1* and reduced cancer metastasis. Oligonucleotide-based drugs have been designed for therapeutic applications concerning lncRNAs because of the abilty to precisely target RNAs.[34]. Therefore, based on our study, *LncDACH1* expression was reduced in lung fibrosis models *in vitro* and *in vivo*, and overexpression of *LncDACH1* alleviated collagen deposition and lung fibroblast overactivation. To further illustrate the protective role of *LncDACH1* in pulmonary fibrosis, we constructed a conserved sequence plasmid of *LncDACH1* containing functional domains, which was consistent with the efficiency of the full-length sequence, and similarly exhibited anti-fibrotic effects in human fetal lung fibroblasts. The discovery of functional domains largely solves the problem of excessively long nucleotide sequences of lncRNAs, which makes *LncDACH1* promising as a lncRNA-targeted drug for pulmonary fibrosis.

There are some limitations to our present study. Although we demonstrated that upregulation of SRSF1 promotes the protein expression and nuclear translocation of β-catenin, we did not determine whether SRSF1 affects the degradation process of *CTNNB1*. Moreover, lncRNA regulates post-translational modification of proteins through ubiquitination, phosphorylation, acetylation and autophagy, thus affecting protein expression level and activity. Wang et al.[35] found that lncRNA *LINRIS* promotes aerobic glycolysis in colorectal cancer by preventing the degradation of *IGF2BP2* through the autophagy−lysosome pathway. Therefore, more comprehensive studies are warranted to determine how lncRNA alter protein levels. As this research was carried out without a pulmonary function test in the therapy experiment, this could be considered a limitation to this study.

5. Conclusions

Our study demonstrates that *LncDACH1* negatively regulates the level of *CTNNB1* by binding to SRSF1 and inhibiting SRSF1 expression, which inhibits the activation of lung fibroblasts and extracellular matrix deposition, thus participating in the process of alleviating lung fibrosis. Therefore, it is possible to utilize replacement of *LncDACH1* to enhance its expression for the prevention and treatment of IPF.

Acknowledgments

We thank Prof. Zhenwei Pan for providing the *LncDACH1*-KO mice and plasmid of *LncDACH1*, and early contributions to the project. This study was supported by the National Natural Science Foundation of China (32171127 and 91949109); the HMU Marshal Initiative Funding (HMUMIF-21023, China); the Major Scientific Fund Project of Heilongjiang Province (ZD2019H001, China); the CAMS Innovation Fund for Medical Sciences (CIFMS, 2019-I2M-5-078, China), the Guangdong Province Basic and Applied Basic Research Fund (2021A1515111049, China), and Postgraduate Research and Practice Innovation Program of HMU (YJSCX2020-15HYD, China).

Author contributions

Haihai Liang and Hongli Shan conceived the project, designed the experiments and edited the manuscript. Jian Sun, Jiayu Guo and Tongzhu Jin planned the experiments, integrated data and wrote the manuscript. Jian Sun, Zhihui Niu, Liangliang Li, Tianyu Li, Huiying Gao and Yuhan Zhang performed cellular and molecular biological experiments and executed the data analysis. Wenxin He and Zhixin Li enrolled patients and collected human samples. Yingying Guo, Tongzhu Jin, Ruoxuan Yang, Qianqian Wang, Wenchao Ma, Wei Su, and Xingxing Fan performed animal studies and analyzed the data.

Conflicts of interest

The authors declared no conflict of interest.

Appendix A. Supporting information

Supporting data to this article can be found online at https://doi.org/10.1016/j.apsb.2022.04.006.

References

1. Liu S, Lv X, Wei X, Liu C, Li Q, Min J, et al. βTRIB3−GSK-3 interaction promotes lung fibrosis and serves as a potential therapeutic target. *Acta Pharm Sin B* 2021;**11**:3105−19.
2. George PM, Spagnolo P, Kreuter M, Altinisik G, Bonifazi M, Martinez FJ, et al. Progressive fibrosing interstitial lung disease: clinical uncertainties, consensus recommendations, and research priorities. *Lancet Respir Med* 2020;**8**:925−34.
3. Liu G, Philp A, Corte T, Travis M, Schilter H, Hansbro N, et al. Therapeutic targets in lung tissue remodelling and fibrosis. *Pharmacol Ther* 2021;**225**:107839.
4. Cameli P, Refini R, Bergantini L, d'Alessandro M, Alonzi V, Magnoni C, et al. Long-term follow-up of patients with idiopathic pulmonary fibrosis treated with pirfenidone or nintedanib: a real-life comparison study. *Front Mol Biosci* 2020;**7**:581828.
5. Li H, Zhao X, Shan H, Liang H. MicroRNAs in idiopathic pulmonary fibrosis: involvement in pathogenesis and potential use in diagnosis and therapeutics. *Acta Pharm Sin B* 2016;**6**:531−9.
6. Zhang X, Hong R, Chen W, Xu M, Wang L. The role of long noncoding RNA in major human disease. *Bioorg Chem* 2019;**92**:103214.
7. Ramnarine V, Kobelev M, Gibb E, Nouri M, Lin D, Wang Y, et al. The evolution of long noncoding RNA acceptance in prostate cancer initiation, progression, and its clinical utility in disease management. *Eur Urol* 2019;**76**:546−59.

8. Wang Y, Fang Z, Hong M, Yang D, Xie W. Long-noncoding RNAs (lncRNAs) in drug metabolism and disposition, implications in cancer chemo-resistance. *Acta Pharm Sin B* 2020;**10**:105−12.
9. Cai B, Ma W, Wang X, Sukhareva N, Hua B, Zhang L, et al. Targeting lncDACH1 promotes cardiac repair and regeneration after myocardium infarction. *Cell Death Differ* 2020;**27**:2158−75.
10. Deng Y, Chen D, Wang L, Gao F, Jin B, Lv H, et al. Silencing of long noncoding RNA Nespas aggravates microglial cell death and neuroinflammation in ischemic stroke. *Stroke* 2019;**50**:1850−8.
11. Jiang X, Zhang F. Long noncoding RNA: a new contributor and potential therapeutic target in fibrosis. *Epigenomics* 2017;**9**:1233−41.
12. Feng M, Tang P, Huang X, Sun S, You Y, Xiao J, et al. TGF-β mediates renal fibrosis *via* the Smad3−Erbb4−IR long noncoding RNA axis. *Mol Ther* 2018;**26**:148−61.
13. Zhao X, Sun J, Chen Y, Su W, Shan H, Li Y, et al. lncRNA PFAR promotes lung fibroblast activation and fibrosis by targeting miR-138 to regulate the YAP1−Twist axis. *Mol Ther* 2018;**26**:2206−17.
14. Dykes I, Emanueli C. Transcriptional and post-transcriptional gene regulation by long non-coding RNA. *Dev Reprod Biol* 2017;**15**:177−86.
15. Cai B, Zhang Y, Zhao Y, Wang J, Li T, Zhang Y, et al. Long noncoding RNA-DACH1 (Dachshund homolog 1) regulates cardiac function by inhibiting SERCA2a (sarcoplasmic reticulum calcium ATPase 2a). *Hypertension* 2019;**74**:833−42.
16. Habermann A, Gutierrez A, Bui L, Yahn S, Winters N, Calvi C, et al. Single-cell RNA sequencing reveals profibrotic roles of distinct epithelial and mesenchymal lineages in pulmonary fibrosis. *Sci Adv* 2020;**6**:eaba1972.
17. Neumark N, Cosme C, Rose K, Kaminski N. The idiopathic pulmonary fibrosis cell Atlas. *Am J Physiol Lung Cell Mol Physiol* 2020;**319**:L887−93.
18. Paz I, Kosti I, Ares M, Cline M, Mandel-Gutfreund Y. RBPmap: a web server for mapping binding sites of RNA-binding proteins. *Nucleic Acids Res* 2014;**42**:W361−7.
19. Cook K, Kazan H, Zuberi K, Morris Q, Hughes T. RBPDB: a database of RNA-binding specificities. *Nucleic Acids Res* 2011;**39**:D301−8.
20. Agostini F, Zanzoni A, Klus P, Marchese D, Cirillo D, Tartaglia G. catRAPID omics: a web server for large-scale prediction of protein−RNA interactions. *Bioinformatics* 2013;**29**:2928−30.
21. Fu Y, Huang B, Shi Z, Han J, Wang Y, Huangfu J, et al. SRSF1 and SRSF9 RNA binding proteins promote Wnt signalling-mediated tumorigenesis by enhancing beta-catenin biosynthesis. *EMBO Mol Med* 2013;**5**:737−50.
22. Cao P, Aoki Y, Badri L, Walker N, Manning C, Lagstein A, et al. Autocrine lysophosphatidic acid signaling activates β-catenin and promotes lung allograft fibrosis. *J Clin Invest* 2017;**127**:1517−30.
23. Noble P, Albera C, Bradford W, Costabel U, Glassberg M, Kardatzke D, et al. Pirfenidone in patients with idiopathic pulmonary fibrosis (CAPACITY): two randomised trials. *Lancet* 2011;**377**:1760−9.
24. Richeldi L, du Bois R, Raghu G, Azuma A, Brown K, Costabel U, et al. Efficacy and safety of nintedanib in idiopathic pulmonary fibrosis. *N Engl J Med* 2014;**370**:2071−82.
25. Song X, Xu P, Meng C, Song C, Blackwell T, Li R, et al. lncITPF promotes pulmonary fibrosis by targeting hnRNP-L depending on its host gene ITGBL1. *Mol Ther* 2019;**27**:380−93.
26. Das S, Krainer A. Emerging functions of SRSF1, splicing factor and oncoprotein, in RNA metabolism and cancer. *Mol Cancer Res* 2014;**12**:1195−204.
27. Möröy T, Heyd F. The impact of alternative splicing *in vivo*: mouse models show the way. *RNA* 2007;**13**:1155−71.
28. Paz S, Ritchie A, Mauer C, Caputi M. The RNA binding protein SRSF1 is a master switch of gene expression and regulation in the immune system. *Cytokine Growth Factor Rev* 2021;**57**:19−26.
29. Sheng J, Zhao Q, Zhao J, Zhang W, Sun Y, Qin P, et al. SRSF1 modulates PTPMT1 alternative splicing to regulate lung cancer cell radioresistance. *EBioMedicine* 2018;**38**:113−26.
30. Pozzi B, Mammi P, Bragado L, Giono L, Srebrow A. When SUMO met splicing. *RNA Biol* 2018;**15**:689−95.
31. Miao J, Liu J, Niu J, Zhang Y, Shen W, Luo C, et al. Wnt/β-catenin/RAS signaling mediates age-related renal fibrosis and is associated with mitochondrial dysfunction. *Aging Cell* 2019;**18**:e13004.
32. Wu Y, Xu L, Cao G, Min L, Dong T. Effect and mechanism of Qingfei Paidu decoction in the management of pulmonary fibrosis and COVID-19. *Am J Chin Med* 2022;**50**:33−51.
33. Sprangers A, Hao L, Banga R, Mirkin C. Liposomal spherical nucleic acids for regulating long noncoding rnas in the nucleus. *Small* 2017;**13**:1602753.
34. Chen Y, Li Z, Chen X, Zhang S. Long non-coding RNAs: from disease code to drug role. *Acta Pharm Sin B* 2021;**11**:340−54.
35. Wang Y, Lu J, Wu Q, Jin Y, Wang D, Chen Y, et al. LncRNA LINRIS stabilizes IGF2BP2 and promotes the aerobic glycolysis in colorectal cancer. *Mol Cancer* 2019;**18**:174.